Int. J. Peptide Protein Res. **31**, 1988, 567–576

Monoclinic polymorph of Boc-Trp-Ile-Ala-Aib-Ile-Val-Aib-Leu-Aib-Pro-OMe(anhydrous)

Parallel packing of 3_{10}-/α-helices and a transition of helix type

ISABELLA L. KARLE,[1] JUDITH L. FLIPPEN-ANDERSON,[1] MUPALLA SUKUMAR[2] and PADMANABHAM BALARAM[2]

[1]*Laboratory for the Structure of Matter, Naval Research Laboratory, Washington, D.C., USA,*
[2]*Molecular Biophysics Unit, Indian Institute of Science, Bangalore, India*

Received 24 September 1987, accepted for publication 8 January 1988

The structures of two crystal forms of Boc-Trp-Ile-Ala-Aib-Ile-Val-Aib-Leu-Aib-Pro-OMe have been determined. The triclinic form (P1, Z = 1) from DMSO/H_2O crystallizes as a dihydrate (Karle, Sukumar & Balaram (1986) *Proc. Natl. Acad. Sci. USA* **83**, 9284–9288). The monoclinic form ($P2_1$, Z = 2) crystallized from dioxane is anhydrous. The conformation of the peptide is essentially the same in both crystal systems, but small changes in conformational angles are associated with a shift of the helix from a predominantly α-type to a predominantly 3_{10}-type. The r.m.s. deviation of 33 atoms in the backbone and C^{β} positions of residues 2–8 is only 0.29 Å between molecules in the two polymorphs. In both space groups, the helical molecules pack in a *parallel* fashion, rather than antiparallel. The only intermolecular hydrogen bonding is head-to-tail between helices. There are no lateral hydrogen bonds. In the $P2_1$ cell, a = 9.422(2) Å, b = 36.392(11) Å, c = 10.548(2) Å, β = 111.31(2)° and V = 3369.3 Å^3 for 2 molecules of $C_{60}H_{97}N_{11}O_{13}$ per cell.

Key words: Aib residues; anhydrous apolar decapeptide; crystal structure; 3_{10}-helix/α-helix transformation; hydrogen bonds

Aggregation of helical, hydrophobic peptides may be an important step in the formation of transmembrane peptide channels (1). The role of specific side chains in promoting helix aggregation is being studied by means of synthetic peptides. The triclinic crystal of Boc-Trp-Ile-Ala-Aib-Ile-Val-Aib-Leu-Aib-Pro-OMe·$2H_2O$, an apolar analog of residues 1–10 of zervamicin IIA, has one molecule of the peptide per cell (2). Since the only mode of repetition in a triclinic cell is by translation in the three axial directions, the packing of the helical columns must necessarily be parallel rather than antiparallel. The parallel packing of α-helices is in contrast to the antiparallel packing generally observed in proteins and in other α-helical peptides (3–5). Consequently, attempts were made to crystallize this decapeptide in a different type of cell by using nonpolar solvents, rather than DMSO/H_2O, which was used to grow the triclinic crystal form. Monoclinic crystals were obtained from wet dioxane, as well as from ethyl acetate/petroleum ether. The latter solvent mixture yielded only poor quality single crystals, although they had the same cell parameters and appeared to have similar intensities for the scattered reflections as

those from dioxane. The monoclinic space group $P2_1$ relates two molecules by a 2-fold screw axis. Thus it was possible to have antiparallel packing of the helices, if the orientation of the helical molecules were perpendicular to the screw axis. Actually the helices lie parallel to the screw axis in the present monoclinic cell and neighboring helices are parallel to each other. The parallel packing of neighboring helices is identical to that found for a 16-residue apolar peptide (6) with the same 1–10 sequence as in the present peptide.

Each of the three molecules with the same 1–10 sequence of residues, and very similar values for conformational angles, contain a different ratio of 3_{10}-helix/α-helix hydrogen bonds ($4 \rightarrow 1/5 \rightarrow 1$) from 1:5 to 4:2.

EXPERIMENTAL PROCEDURES

Boc-Trp-Ile-Ala-Aib-Ile-Val-Aib-Leu-Aib-Pro-OMe was synthesized by conventional solution-phase procedures and crystals were grown by slow evaporation from wet dioxane. A dry crystal in the form of a somewhat irregular rhomboid, $0.10 \times 0.12 \times 0.18$ mm, was used for X-ray data collection on an automated four-circle diffractometer with CuKα radiation and a graphite monochromater ($\lambda = 1.54178$ Å). The θ–2θ scan technique was used with a 2.0° scan, variable scan rate of 7° to 30°/min, and $2\theta_{max} = 100°$, for a total of 3556 independent reflections and 3020 reflections with intensities $> 3\sigma(F)$ to a resolution of 1.0 Å. Three reflections, 3 0 0, 0 8 0 and 0 2 4, monitored after every 60 measurements, were constant within 2%.

Lorentz and polarization corrections were applied to the data. The space group is $P2_1$ with a = 9.422(2) Å, b = 36.392(11) Å, c = 10.548(2) Å, $\beta = 111.31(2)°$, V = 3369.3 Å, Z = 2 and $d_{calc} = 1.163$ g/cm^3 based on a formula weight of 1180.51 for $C_{60}H_{97}N_{11}O_{13}$ (anhydrous).

It was expected that the molecule would have a conformation similar to that found for the same substance in a P1 cell (2). Accordingly, a fragment of 33 atoms, containing the backbone and C^β atoms in residues 2–8 from ref. (2), was used as a model in the vector search procedure in the PATSEE computer program (7) contained in the SHELX84 package of programs (8). The orientation of the fragment in the monoclinic cell and the translation to the correct position with respect to the cell axes were readily obtained only after the normalized $|E_{hkl}|$ values (9) were obtained from the raw data by processing with the XTAL86 program (10) rather than the SHELX84 program (8). The remainder of the atoms in the molecule were found with the partial structure procedure (11).

Full-matrix, anisotropic least-squares refinement was performed on the C, N and O atoms before hydrogen atoms (those bonded to C atoms) were added in idealized position. Then refinement was continued with block-diagonal least-squares alternately on blocks of residues 1–5 (480 parameters) and 6–10 (364 parameters) with the hydrogen atoms riding on the atoms to which they are bonded and their isotropic thermal factors fixed $\simeq U_{eq}$ of the bonded C atoms. Hydrogen atoms bonded to the N atoms were located in difference maps and their coordinates were refined with U_{iso} fixed as above (SHELXTL program). The final agreement factors were R = 0.063 and Rw = 0.055.

Fractional coordinates for the refined atoms are listed in Table 1, a view of the molecule is shown in Fig. 1, torsional angles are listed in Table 2, and hydrogen bonds are shown in Table 3.

RESULTS

Molecule

The conformation of the decapeptide molecule in the two different space groups, P1, $P2_1$, is essentially the same, as can be seen by the superposition of the molecules in Fig. 2. The average fit of back-bone atoms and C^β atoms in residues 2–8 is 0.29 Å. The largest deviation between two equivalent backbone atoms in the two molecules is 1.1 Å between the $C'10$ atoms at the *C*-terminal. The hexadecapeptide with the same 1–10 sequence (6) also has the same conformation for the residues 1–9. Torsional angles ϕ ($N_i - C_i^\alpha$) and ψ ($C_i^\alpha - C_i'$) in the three molecules are compared in Fig. 3. They can be compared only

TABLE 1

Atomic coordinates ($\times 10^4$) *and equivalent isotropic displacement parameters* (Å^2 $\times$ 10^3)

	x	y	z	*U_{eq}
C(2)	5690(11)	3000(3)	3982(8)	71(4)
C(3)	6149(14)	3393(3)	4292(11)	116(6)
C(4)	7043(12)	2763(3)	4696(9)	95(5)
C(5)	4259(11)	2908(3)	4288(10)	101(5)
O	5360(6)	2990	2491(5)	69(3)
C′(0)	5061(9)	2672(3)	1842(9)	62(4)
O(0)	4755(7)	2383(2)	2298(6)	77(3)
N(1)	5083(8)	2697(2)	569(7)	59(3)
C$^{\alpha}$(1)	4581(10)	2389(2)	−363(7)	58(4)
C′(1)	5445(11)	2042(2)	143(9)	58(4)
(1)	4870(7)	1737(2)	−176(6)	78(3)
C$^{\beta}$(1)	4660(10)	2488(2)	−1733(7)	73(4)
C$^{\gamma}$(1)	6270(10)	2546(3)	−1756(8)	61(4)
C$^{\delta}$(11)	7010(12)	2870(2)	−1580(8)	67(5)
C$^{\delta}$(12)	7223(11)	2283(2)	−1993(8)	60(4)
N$^{\varepsilon}$(11)	8401(11)	2825(2)	−1641(7)	75(4)
C$^{\varepsilon}$(12)	8558(12)	2466(3)	−1931(8)	69(5)
C$^{\varepsilon}$(13)	7135(12)	1901(3)	−2271(9)	78(5)
C$^{\zeta}$(11)	9754(12)	2289(3)	−2159(8)	79(5)
C$^{\zeta}$(12)	8339(16)	1729(3)	−2484(9)	99(6)
C$^{\eta}$(1)	9616(15)	1923(4)	−2425(10)	96(6)
N(2)	6918(9)	2073(2)	1008(8)	58(3)
C$^{\alpha}$(2)	7873(9)	1764(2)	1536(8)	60(4)
C′(2)	7249(10)	1504(3)	2332(8)	65(4)
O(2)	7532(6)	1171(2)	2408(5)	76(3)
C$^{\beta}$(2)	9517(9)	1869(2)	2359(8)	68(4)
C$^{\gamma}$(21)	9656(10)	2092(3)	3636(9)	86(5)
C$^{\gamma}$(22)	10257(11)	2067(3)	1496(10)	93(5)
C$^{\delta}$(2)	11190(12)	2161(4)	4611(12)	140(7)
N(3)	6341(9)	1655(2)	2932(7)	67(3)
C$^{\alpha}$(3)	5697(11)	1423(2)	3752(9)	73(4)
C′(3)	4724(11)	1127(3)	2894(10)	66(5)
O(3)	4744(7)	807(2)	3348(6)	89(3)
C$^{\beta}$(3)	4753(11)	1666(3)	4344(9)	88(5)
N(4)	3750(9)	1213(2)	1655(9)	83(4)
C$^{\alpha}$(4)	2678(12)	957(3)	723(11)	96(5)
C′(4)	3540(14)	638(3)	420(10)	90(6)
O(4)	3056(9)	325(2)	315(10)	148(6)
C$^{\beta}$(41)	1494(12)	830(3)	1315(14)	125(7)
C$^{\beta}$(42)	1901(14)	1161(3)	−609(11)	134(7)
N(5)	4884(11)	708(2)	292(8)	79(4)
C$^{\alpha}$(5)	5740(12)	433(3)	−65(9)	75(5)
C′(5)	6540(10)	182(3)	1158(9)	72(4)
O(5)	6589(7)	−155(2)	984(6)	88(3)
C$^{\beta}$(5)	6896(13)	609(3)	−622(10)	100(6)
C$^{\gamma}$(51)	6091(20)	866(3)	−1874(17)	164(11)
C$^{\gamma}$(52)	7865(16)	303(3)	−966(13)	144(9)
C$^{\delta}$(5)	4870(23)	695(4)	−2987(14)	211(13)
N(6)	7235(7)	344(2)	2344(7)	66(3)
C$^{\alpha}$(6)	8017(11)	121(3)	3500(9)	82(4)
C′(6)	6981(15)	−157(3)	3795(9)	80(5)
O(6)	7491(8)	−471(2)	4216(6)	98(3)
C$^{\beta}$(6)	8730(12)	380(3)	4805(10)	105(5)
C$^{\gamma}$(61)	10052(13)	601(3)	4577(12)	142(7)
C$^{\gamma}$(62)	9364(16)	176(3)	6012(12)	160(8)
N(7)	5543(12)	−66(2)	3580(8)	75(4)
C$^{\alpha}$(7)	4414(13)	−303(3)	3840(10)	90(6)
C′(7)	4193(11)	−662(3)	3033(11)	86(5)
O(7)	3754(10)	−939(2)	3431(7)	128(5)
C$^{\beta}$(71)	2941(13)	−102(3)	3363(13)	128(8)
C$^{\beta}$(72)	5047(17)	−402(3)	5397(12)	152(9)
N(8)	4443(8)	−651(2)	1854(8)	69(3)
C$^{\alpha}$(8)	4237(10)	−971(2)	991(9)	69(4)
C′(8)	5493(10)	−1242(3)	1380(9)	61(4)
O(8)	5327(6)	−1552(2)	881(6)	76(3)
C$^{\beta}$(8)	3856(10)	−859(2)	−472(10)	87(5)
C$^{\gamma}$(8)	2165(17)	−751(3)	−1376(14)	144(9)
C$^{\delta}$(81)	1547(13)	−463(3)	−794(13)	131(7)
C$^{\delta}$(82)	2114(21)	−659(5)	−2787(14)	256(13)
N(9)	6852(9)	−1125(2)	2257(8)	71(4)
C$^{\alpha}$(9)	8258(10)	−1341(3)	2628(10)	78(5)
C′(9)	8394(9)	−1505(3)	1298(11)	77(5)
O(9)	8666(7)	−1830(2)	1218(7)	95(3)
C$^{\beta}$(91)	9622(10)	−1087(3)	3371(11)	113(5)
C$^{\beta}$(92)	8259(11)	−1642(3)	3555(11)	110(6)
N(10)	8206(7)	−1279(2)	258(9)	77(4)
C$^{\alpha}$(10)	8175(10)	−1430(2)	−1080(10)	83(5)
C′(10)	9716(13)	−1559(3)	−943(13)	82(6)
O(10)	10905(8)	−1483(2)	−27(8)	89(3)
C$^{\beta}$(10)	7654(13)	−1115(3)	−2095(12)	142(6)
C$^{\gamma}$(10)	7375(15)	−802(3)	−1409(14)	135(8)
C$^{\delta}$(10)	8115(11)	−868(3)	147(12)	104(6)
C(11)	11125(15)	−1859(3)	−2090(14)	147(8)
O(11)	9635(9)	−1754(2)	−2042(7)	111(4)

*$U_{eq} = \frac{1}{3}\Sigma\Sigma\ U_{ij} a_i^* a_j^* (a_i \cdot a_j)$.

through residue 8, since in the two decapeptide molecules, there is a change in the signs of the ϕ, ψ values at C$^{\alpha}$(9).

Although the ϕ, ψ values are very similar in the three molecules, the number of 3_{10}-type (4 → 1) hydrogen bonds as compared to the number of α-helical (5 → 1) hydrogen bonds is quite different in the three molecules. The ratio for the two kinds of hydrogen bonds is 1:5 for the decapeptide in P1 (*A*), 2:4 for the 1–10 region in the hexadecapeptide (*B*), and 4:2 for the decapeptide in P2_1 (*C*). In Fig. 3, the ψ values are arranged in *A*, *B*, *C* order with A being the lowest graph and having the largest number of 5 → 1 hydrogen bonds, consistent with the ideal ψ values for α-helices. For the ϕ values, *A*, *B* and *C* are

TABLE 2

Conformational angles[a] for monoclinic polymorph

	1 Trp	2 Ile	3 Ala	4 Aib	5 Ile	6 Val	7 Aib	8 Leu	9 Aib	10 Pro
ϕ	−58.3[b]	−58.8	−60.5	−59.1	−75.7	−58.6	−58.0	−80.8	45.8	−70.1
ψ	−28.9	−27.6	−44.1	−37.5	−45.2	−35.6	−28.3	−17.1	49.7	168.5[c]
ω	−178.5	−179.0	−177.2	−176.4	−178.8	−178.9	−178.5	−172.6	−174.1	173.1[d]
χ'	67.4	63.3			−56.6	−69.4		−81.6		−0.9
		−62.5			178.2	172.9				
χ^2	−92.1	170.8			−54.6			55.4		15.3
	89.7							−178.8		
χ^3										−23.6
χ^4										22.7
$C^\delta NC^\alpha C^\beta$										−14.3

The torsion angles for rotation about bonds of the peptide backbone (ϕ, ψ, and ω) and about bonds of the amin acid side chains (χ) are described in ref. 12.

[a] E.s.d.'s ~ 1.0°.

[b] C′(0) N(1) C^α(1) C′(1).

[c] N(10) C^α(10) C′(10) O(OMe).

[d] Cα(10) C′(10) O(OMe) C(OMe).

TABLE 3

Hydrogen bonds

Type	Donor	Acceptor	Length, Å	Angle, degs. (C = O. . .N)
Intermolecular	N^ε(11)[a]	O(9)	2.918	128
(head-to-tail		O(10)	3.005	103
	N(1)	O(8)	3.085	176
Intramolecular[b]				
(4 → 1)	N(3)	O(0)	2.995	132
(4 → 1)	N(4)	O(1)	3.155	126
(5 → 1)	N(6)	O(2)	3.019	164
(5 → 1)	N(7)	O(3)	3.255	155
(4 → 1)	N(8)	O(5)	3.088	118
(4 → 1)	N(9)	O(6)	3.065	121

[a] Bifurcated hydrogen bond.

[b] The N(5). . .O(2) distance is 3.161 Å, reasonable for a hydrogen bond; however, the H(N5). . .O(2) distance is 2.8 Å, indicating that the hydrogen atom is not directed toward the O(2) atom.

arranged in reverse order, however, the differences are significant only for residue 5. The difference for the ideal values of ϕ for 3_{10}- and α-helices is small.

The values of the lengths and angles of covalent bonds are very similar in all three structures. It is interesting to observe that small changes in ϕ, ψ values (3–9°), in a 3_{10}-/α-helix, can cause sufficient distance or direction changes to result in switching hydrogen bonds to different NH and O atoms. In *A*, N(4) and O(6) are not involved in intramolecular hydrogen bonding, in *B*, N(5) and O(6), whereas in *C*, N(5) and O(4). The non-

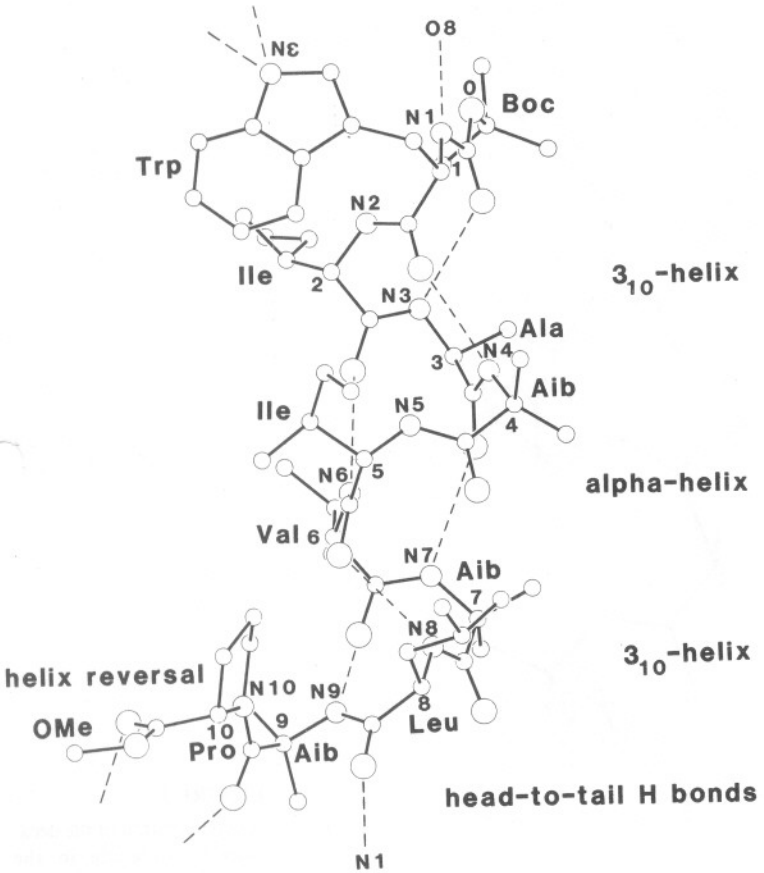

FIGURE 1

View along the helix of the decapeptide molecule drawn by computer using the experimentally determined coordinates in the monoclinic crystal. The C^{α} atoms are labeled 1–10. The number 0 is at the position of an O atom in the Boc group. Hydrogen bonds are indicated by dashed lines.

participating NH or O atoms occur at boundaries between 4 → 1 and 5 → 1 hydrogen bonds. The hydrogen bonds in *C* are listed in Table 3 and are shown in Fig. 1.

Among the side chains, the only significant conformational change is in the Ile[2] residue where the longer branch has g^-, t and the shorter branch g^+ conformations both in the present structure and in the 16-residue peptide, whereas in the decapeptide in P1 the longer branch is t, g^- and the shorter branch is g^-. For Ile[5], the conformation is the same in all three structures, i.e. g^+, t and g^+ for the longer and shorter branches, respectively; but different than the two conformations observed for Ile[2].

Packing

The long dimension of the unique axis *b*, 36.39 Å, and the small cross-section of the unit cell, 9.42 × 10.55 Å, indicated immediately that the two helical molecules in the cell, related by a 2-fold screw, must be stacked over each other in the *b* direction. Perpendicular to the helix direction, the molecules repeat only by translation (Fig. 4). In this structure also, the packing of the helices is in the *parallel* mode, as it has been in the polymorph in P1 (2) and the 16-residue peptide in P1 (6). In fact, the parallel packing of molecules shown in Fig. 4 is very similar to that occurring for the 1–9 residues (upper part) in the 16-residue peptide shown in Fig. 5. There are four lateral C. . .C approaches of ~3.5 Å, three of them with the tryptophanyl side-chain and C(4), C^{β}(42) and C^{β}(3). Almost all other lateral approaches between molecules are > 3.8 Å.

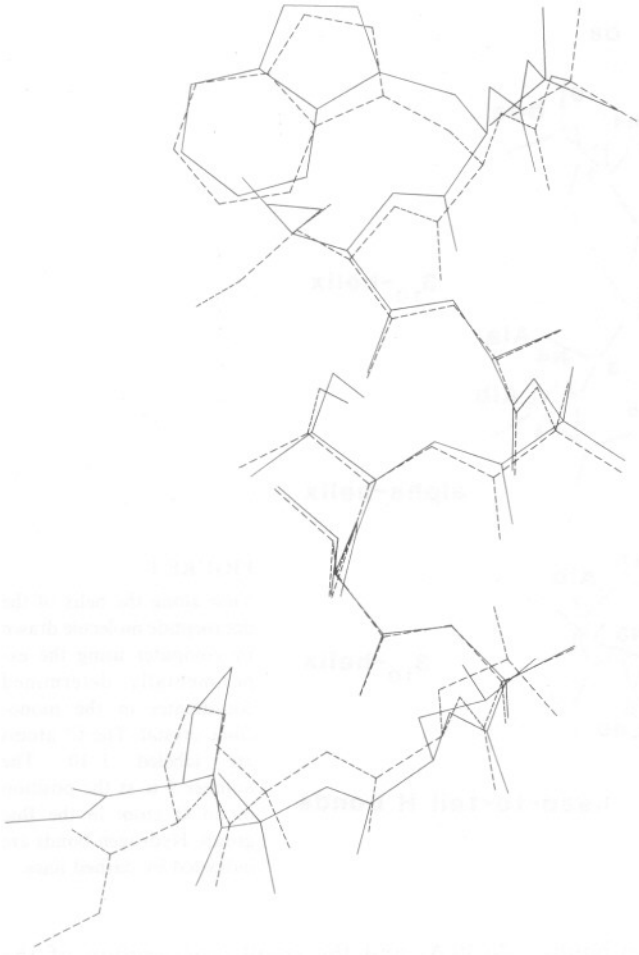

FIGURE 2
A superposition of the decapeptide molecule in the monoclinic cell (——lines) with the same molecule in the triclinic cell (– – –lines).

Intermolecular hydrogen bonds

The only intermolecular hydrogen bonds are the head-to-tail type between N(1). . .O(8) (1 − x, 1/2 + y, −z) and N^{ε}(11). . .O(9) and O(10) (2 − x, 1/2 + y, −z), (Fig. 4). In all three structures referred to in this paper, N(1) and N^{ε}(11) of the tryptophanyl residue participate in head-to-tail hydrogen bonds, either directly or mediated by a water molecule. In the other two structures, N(2) forms a hydrogen bond to a water molecule. In the present structure, there is no evidence for a solvent of crystallization, even at partial occupancy, and N(2) does not participate in any hydrogen bonding. A search of the space above N(2), near x = 0.81, y = 0.28 and z = 0.05, shows that if a water molecule were placed there, it would be too close to the C atom of OMe from a neighboring molecule.

DISCUSSION

The structures of the two crystalline forms of the decapeptide establish that minor changes in backbone torsion angles can result in a transition from a 3_{10}-helical (4 → 1) to an α-helical (5 → 1) hydrogen bonding scheme. The N– – –O distances and C = 0– – –N angles, corresponding to potential 4 → 1 and 5 → 1 hydrogen bonds, for the first 9 residues of the two decapeptide forms and the hexadecapeptide are compared in Table 4. The hydrogen bonding patterns in the three structures are schematically compared in Fig. 6.

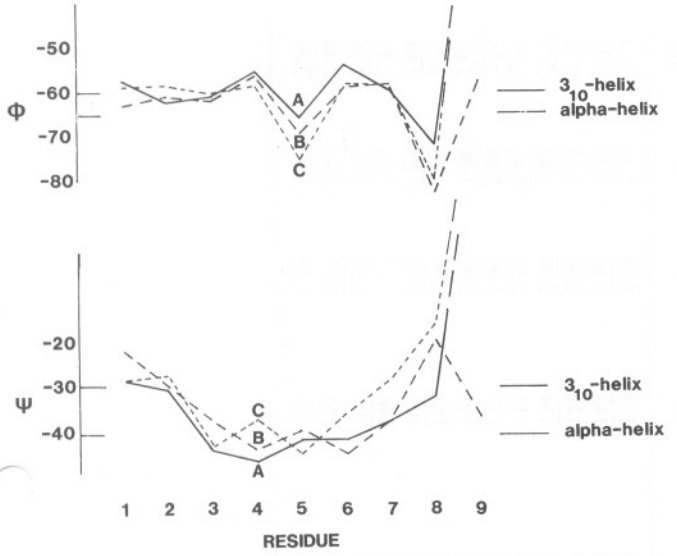

FIGURE 3

A comparison of the ϕ values (upper graph) and ψ values (lower graph) in the decapeptide in P1 (A), residues 1–9 in the hexadecapeptide in P1 (B) and the decapeptide in $P2_1$ (C).

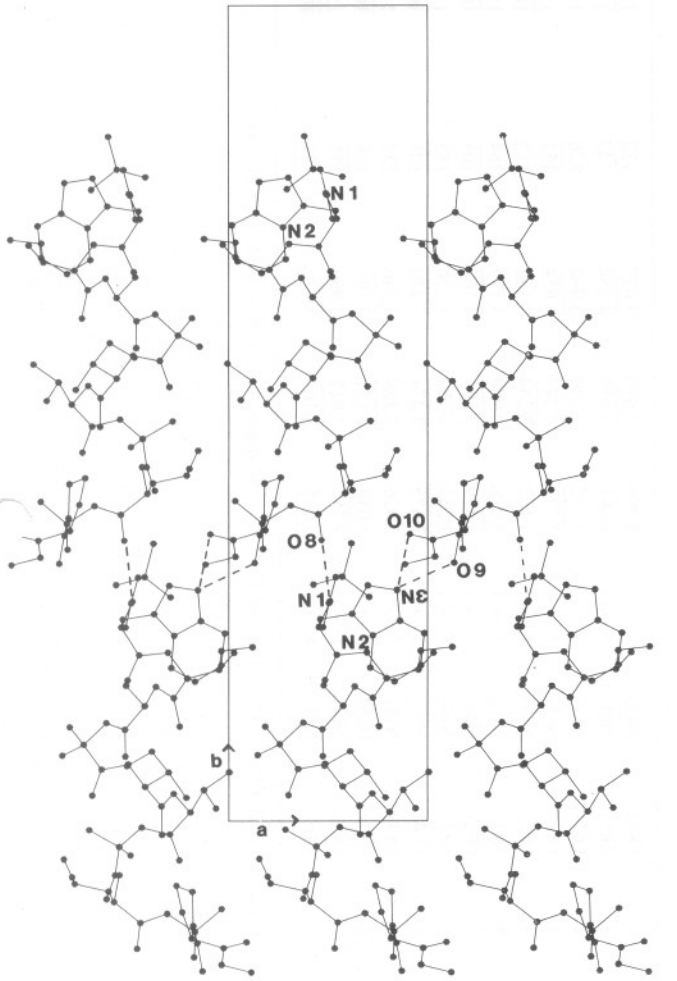

FIGURE 4

Packing of the decapeptide molecule in the $P2_1$ cell and neighboring molecules in two adjacent cells. The *c* axial direction is up from the page. Intermolecular, head-to-tail, hydrogen bonds are indicated by dashed lines.

TABLE 4

Comparison of N. . .O distances[a], C = O. . .N angles and H. . .O distances, corresponding to potential 4 → 1 and 5 → 1 hydrogen bonds, for the first nine residues of the monoclinic decapeptide (I), triclinic decapeptide (II) and hexadecapeptide (III). The value for hydrogen bonds chosen for each structure are underlined

	Acceptor	Donor	Type	N. . O I	N. . O II	N. . O III	C = Ô. . .N I	C = Ô. . .N II	C = Ô. . .N III	H. . O I	H. . O II	H. . O III
1.	O(0)	N(3)	4 → 1	2.995	3.010	3.027	132	130	133	2.16	2.36	2.14
2.	O(0)	N(4)	5 → 1	4.361	3.959	4.254	147	150	143	3.85	3.27	3.42
3.	O(1)	N(4)	4 → 1	3.155	3.130	3.040	126	119	121	2.30	2.53	2.34
4.	O(1)	N(5)	5 → 1	3.777	3.247	3.654	152	159	154	2.94	2.48	2.77
5.	O(2)	N(5)	4 → 1	3.162	3.244	3.139	112	104	113	2.53	2.81	2.51
6.	O(2)	N(6)	5 → 1	3.019	2.960	3.175	164	157	157	1.99	2.09	2.27
7.	O(3)	N(6)	4 → 1	3.359	3.361	3.168	105	104	109	2.92	3.08	2.65
8.	O(3)	N(7)	5 → 1	3.255	3.170	3.170	155	155	159	2.54	2.28	2.23
9.	O(4)	N(7)	4 → 1	3.675	3.474	3.430	101	106	105	3.30	3.03	2.94
10.	O(4)	N(8)	5 → 1	3.926	3.189	3.346	139	152	148	3.17	2.45	2.51
11.	O(5)	N(8)	4 → 1	3.088	3.131	3.191	118	108	108	2.25	2.66	2.56
12.	O(5)	N(9)	5 → 1	3.756	3.012	2.965	151	158	158	2.87	2.46	2.44
13.	O(6)	N(9)	4 → 1	3.065	3.169	3.170	121	109	108	2.33	2.19	2.30

[a] E.s.d.'s: 0.01 Å for N. . O, < 1.0° for C = O. . .N angles, and 0.10 − 0.15 Å for H. . O.

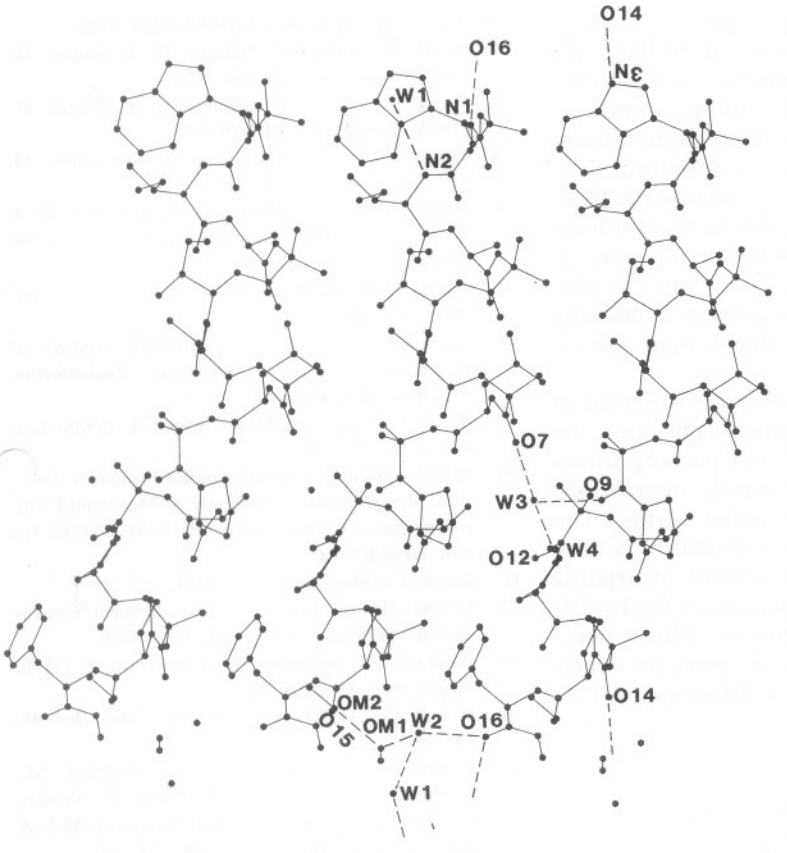

FIGURE 5
Packing of neighboring molecules of the 16-residue peptide (6). Compare with Fig. 4.

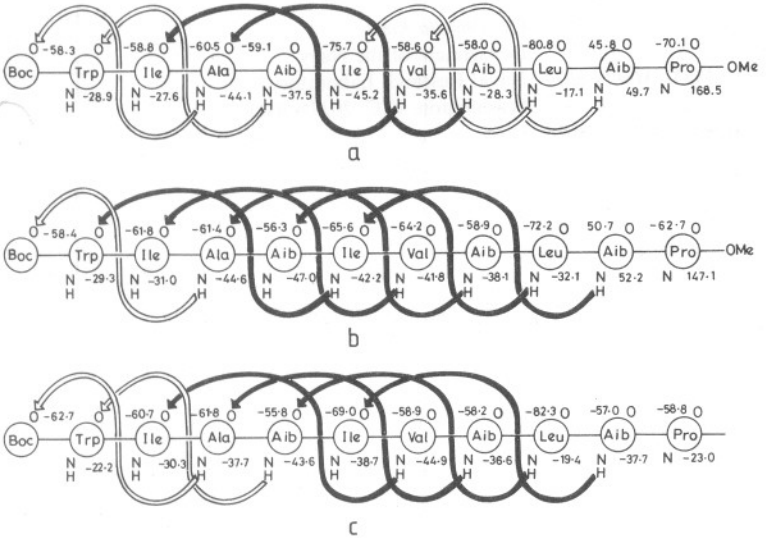

FIGURE 6
Schematic hydrogen bonding patterns in the crystal structure of (a) the decapeptide, $P2_1$, (b) the decapeptide, P1 and (c) the first nine residues of the hexadecapeptide, P1. The dark arrows indicate $5 \rightarrow 1$ hydrogen bonding while the light arrows indicate $4 \rightarrow 1$ hydrogen bonding. ϕ (top), ψ (bottom) values at each residue are indicated.

These observations suggest that n.m.r. studies aimed at delineating the nature of hydrogen bonded NH groups are necessarily limited by the possibility of similar conformational interconversions in solution, which may occur rapidly on the n.m.r. timescale. Indeed, spectral data for helical Aib containing decapeptides have been interpreted in terms of solvent dependent transitions between 3_{10}- and α-helical structures (13). This may be particularly important for sequences containing relatively few, stereochemically rigid Aib residues.

The parallel packing of helices observed in the two decapeptide polymorphs and the hexadecapeptide suggest that packing forces other than helix dipole-dipole interactions (14) stabilize these crystalline forms. The packing of helices in these structures is relatively loose, resulting in solvent incorporation into cavities or the presence of voids with greater than atomic dimensions. This is reminiscent of helix packing in proteins which results in the formation of defect spaces (15, 16).

ACKNOWLEDGMENTS

This work was supported in part by National Institutes of Health Grant GM30902 and in part by a grant from the Department of Science and Technology, India.

REFERENCES

1. Mathew, M.K. & Balaram, P. (1983) *Mol. Cell. Biochem.* **50,** 47–64
2. Karle, I.L., Sukumar, M. & Balaram, P. (1986) *Proc. Natl. Acad. Sci. USA* **83,** 9284–9288
3. Bosch, R., Jung, G., Schmitt, H. & Winter, W. (1985) *Biopolymers* **24,** 961–978
4. Bosch, R., Jung, G., Schmitt, H. & Winter, W. (1985) *Biopolymers* **24,** 979–999
5. Richardson, J.S. (1981) *Adv. Protein Chem.* **34,** 167–339
6. Karle, I.L., Flippen-Anderson, J., Sukumar, M. & Balaram, P. (1987) *Proc. Natl. Acad. Sci. USA* **84,** 5087–5091
7. Egert, E. & Sheldrick, G.M. (1985) *Acta Cryst.* **A41,** 262–268
8. MicroVAX version of SHELXTL system of programs, Nicolet Analytical Instruments, Madison, Wisconsin
9. Karle, J., Hauptman, H. & Christ, C.L. (1958) *Acta Cryst.* **11,** 757–761
10. XTAL System of Crystallographic Programs, Tec nical Report 1364.2 University of Maryland Computer Science Center, College Park, MD 20742, 3rd edn., March 1986
11. Karle, J. (1968) *Acta Cryst.* **B24,** 182–186
12. IUPAC-IUB Commission on Biochemical Nomenclature (1970) *Biochemistry* **9,** 3471–3479
13. Balaram, H., Sukumar, M. & Balaram, P. (1986) *Biopolymers* **25,** 2209–2223
14. Hol. W.G.J. (1985) *Progr. Biophys. Mol. Biol.* **45,** 149–195
15. Frauenfelder, H., Hartmann, H., Karplus, M., Kuntz, Jr. I.D., Kuriyan, J., Parak, F., Petsko, G.A., Ringe, D., Tilton, Jr. R.F. Connolly, M.L. & Max, N. (1987) *Biochemistry* **26,** 254–261
16. Gekko, K. & Hasegawa, Y. (1986) *Biochemistry* **25,** 6563–6571

Address:

Dr. *Isabella Karle*
Department of the Navy
Naval Research Laboratory
Washington, D.C. 20375-5000
USA